

Non-linear Self-Exited Resonant Bolometer

Dmitry Anatolyevich Kovriguine
Industrial Engineering Institute. Russian Academy of Sciences
Belinskogo str., 85 Nizhny Novgorod 603024, Russia
kovriguineda@gmail.com

Abstract

A self-excited resonant bolometer refers to a perspective measurement tool intended for detecting weak infrared electromagnetic signals. The physics of the resonant bolometer is based on a transform of the radiation energy into the thermal one with the help of a heat-sensitive element integrated into a high-quality resonant RLC-circuit. Self-excited oscillations in this resonant circuit are supported due to a low-noise generator operating accordingly to the properties of a Josephson junction. This paper proposes a nonlinear mathematical model of the self-excited resonant bolometer which corresponds to conventional physical and material parameters already reached in nanotechnologies. The model can be of interest both for researchers and designers on the area of high-precision equipments, for instance, associated with q-bit readout problems, as well. The noise evaluation, by the sensitivity of the resonant bolometer, is evaluated as $10E-13$ W by the incoming power.

Key Word and Phrases

Non-linear Bolometer, Infrared Radiation, Josephson Junction, Transition Edge Sensor, Self-Excited Oscillations, RLC-Circuit.

1. Introduction

Recent cosmology experiments have revealed an accelerated expansion of the Universe and anisotropies in the Cosmic Microwave Background radiation. There are known several cosmology instruments such as balloon telescope BOOMERanG, OLIMPO, B-POL etc., trying to detect the relict waves caused by Big Bang. The experimental observations inspire novel challenges in theoretical scenarios based on accurate measurements using modern ultra-sensitive detectors. The resonant bolometer, proposed as a mathematical model in the present paper, seems to be one of such promising tools. Moreover, analogous superconducting devices have showed some promising routes to quantum computations in the recent years.

We study a model of the resonant bolometer, whose functioning is based on a conversion of the electromagnetic radiation energy into the thermal one by a heat-sensitive element integrated into the high-quality resonant circuit. Self-excited oscillations in the resonant circuit are supported by a low-noise generator acting periodically, accordingly to the physical properties of a Josephson junction. The heat-sensitive element implemented into the resonant circuit passes from the superconducting state to the resistive one under the incoming pulse. The operating temperature of all the sensitive parts of the bolometer is supposed to be set slightly below the superconducting edge. This means that the self-excited electric oscillations provide a certain portion of the heat to support the temperature of the bolometer near the operating regime. The measurement procedure has to identify changes in the amplitude and phase modulation at the absorption of incoming infrared signals. The main objective of this study is to provide one more idea for the accurate identifying the weak electromagnetic radiation. The sensitivity of this sensor at conventional material parameters may be evaluated as about $10E-13$ W by the input power.

From a viewpoint of the theory oscillations, the self-excited resonant bolometer can be treated as a self-excited oscillatory system possessing more than single degrees of freedom. In spite of some complexity in the analytical description, since the governing equations appear as essentially nonlinear ones, the numerical modeling leads to a conclusion that this system is extremely simple, because any chaotic motion inherent in complex nonlinear dynamical systems, has no place at all. Point out that this is a fairly rare case in the theory of oscillations. This means that, on the one hand, we have got a standard self-excited system characterized by a simple dynamics. On the other hand, the model of the self-excited resonant bolometer possesses a negative feedback which

provide most optimal conditions allowing for a quickest cooling of the sensor. This can lead to a technical result which improves the sensitivity, accuracy and stability by reducing the measurement errors up to the level limited almost by thermal fluctuations. This creates perspectives for more efficient identification of unknown parameters of the incoming electromagnetic radiation.

Mathematically, the model of the resonant bolometer is represented by a set of four essentially nonlinear ordinary differential equations which cannot be effectively studied by the perturbation methods developed mainly for quasi-linear dynamical systems in more details. The first pair of these equations describes effects of phase transition through the Josephson junction, as a superconductor possessing an extremely small isolating gap, and electric oscillations in the high-quality RLC-circuit connected in parallel to this junction. The second pair of equations controls thermal processes during the Josephson generation in the junction, and the absorption of external microwave signals by the sensitive resistive element integrated into the RLC-circuit. Nonetheless, the idle operating regime of the resonant bolometer is satisfactory evaluated by elemental approach, since the governing equations are almost decoupled in this case. This waiting regime exhibits an extremely sharp response in the resonantly tuned RLC-circuit due to the Josephson generation. Though, it seems to be true that processes accompanied by the signal absorption may be investigated numerically only, in particular, because of strong temperature dependences in the coefficients entering the equations of motion.

We should note, today all the conventional bolometers almost always operate using a DC biasing. These are linear systems investigated by the tools of spectral methods. Therefore, there is no any reason to invite the modern theory of nonlinear oscillations in the study. This probably is caused, on the one hand, by an attractive simplicity of the set-up, while on the other hand, by the possibilities of nanotechnologies developed up to now, which always try to find routes to modify the existing sensors in order to be closer to ideal properties predicted by the simple theory of electricity. A number of recent actual studies [1–5] deal with the periodically forced models, based on approaches inherent in nonlinear dynamical systems with resonances. The periodical pumping is modeled therein just as trigonometric functions. Although, we should not forget, such a pumping represents a power source of parasite noises in practice, following the physical properties of any conventional generator of periodical signals. The present paper try to overcome such a deficiency by combining the DC biasing with the periodical pumping due to the self excitation mechanism inside the cooled system.

Finally, the fast development in the nanotechnologies makes us supposing that the dynamical sensors will really take place soon instead traditional sensors with the DC biasing.

2. Josephson-type generator loaded in parallel with the resonant RLC-circuit

Consider a Josephson junction across which a constant DC current i passes. Let us neglect heat effects, then the equations describing the Josephson generation holds true [6–8]:

$$C\dot{v} + v/\rho + J \sin \varphi = i, \quad \dot{\varphi} = 2ev/\hbar \quad (2.1)$$

where $v(t)$ is the voltage across the contact; $\varphi(t)$ is the so-called Josephson's phase; J denotes the critical current; e stands for the absolute value of the electron charge; \hbar is the Planck's constant; C and ρ are the capacitance and junction resistance, respectively; points denote differentiation with respect to the time t . It is known that if the current through the Josephson junction is less than its critical value, $i < J$, then there is no generation of oscillations [9, 10]. In this case stationary values of the Josephson's transition phase φ_0 are determined by a simple equation: $J \sin \varphi_0 = i$. The generation of oscillations appears when the current through the Josephson junction exceeds the critical value, i.e. $i \geq J$.

Now let us to load this Josephson generator by a high-quality RLC-circuit connected in parallel to the Josephson junction. The system also operates by applying a DC bias (Fig. 1). The symbol JJ denotes the Josephson junction in this figure.

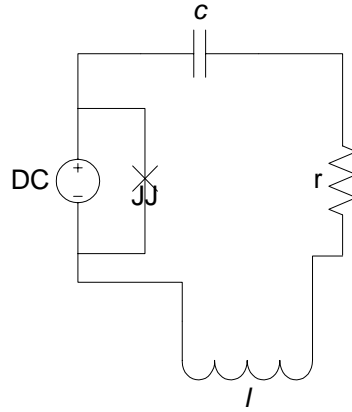


Fig. 1 Josephson's generator connected in parallel to the RLC-circuit.

Following this scheme, the dynamical system reads:

$$C\dot{v} + v/\rho + J \sin \varphi = i - j; \quad \dot{\varphi} = 2ev/\hbar;$$

$$V_{TES} h_{TES} \dot{T} = rj^2(t) - V_{TES} \Sigma_{TES} [T^n - (T_s - \Delta T)^n] \quad (2.2)$$

$$V_{JJ} h_{JJ} \dot{\Theta} = (i - j)v - V_{JJ} \Sigma_{JJ} [\Theta^n - (T_s - \Delta T)^n]$$

$$lj + q/c + rj = v; \quad \dot{q} = j.$$

where V_{TES} is the volume of the absorber associated with the heat-sensitive element; $h_{TES} = h_{TES}(T)$ is the specific heat function of the absorber; Σ_{TES} stands for the coefficient of thermal conductivity, the empirical constant $n=5$ originates from the theory [9]; $T(t)$ is the temperature of the heat-sensitive element; $T_s - \Delta T$ denotes the constant temperature of the coolant tank; ΔT is the average controlled temperature near the operating point, appearing due to small electric oscillations in the resonant circuit. The parameters of the superconducting junction are the following: V_{JJ} is the volume of the junction; Σ_{JJ} is the coefficient of thermal conductivity; $\Theta(t)$ is the Josephson junction temperature; $h_{JJ} = h_{JJ}(\Theta)$ stands for the specific heat function; $q(t)$ and $j(t)$ are the charge and current in the resonant circuit, respectively. The resonant circuit possesses typical parameters of the inductance l , capacitance c and resistance r . All the remaining symbols are the same as previously.

The value of the critical current in the junction near the critical temperature is defined by the following formulae [11, 12]:

$$J = \frac{\pi}{2e\rho} \Delta \tanh\left(\frac{\Delta}{k_B \Theta}\right); \quad \Delta = 3.52 k_B T_{c,JJ} \sqrt{1 - \frac{\Theta}{T_{s,JJ}}}.$$

in which Δ is the energy gap of the superconductor as the function of the temperature $\Theta(t)$; $T_{s,JJ}$ is the value of the critical temperature; k_B denotes the Boltzmann constant. To obtain the dependence of the energy gap Δ upon the temperature $\Theta(t)$, one should solve a somewhat difficult integral equation [11]. However, the behavior of this dependence is simple enough; if $\Theta = 0$, then $2\Delta/k_B T_{s,JJ} \approx 3.52$, else if $\Theta \geq T_{s,JJ}$, then $\Delta = 0$ (Fig. 2). This means that the junction turns into a standard resistance of the constant value ρ at ambient temperatures.

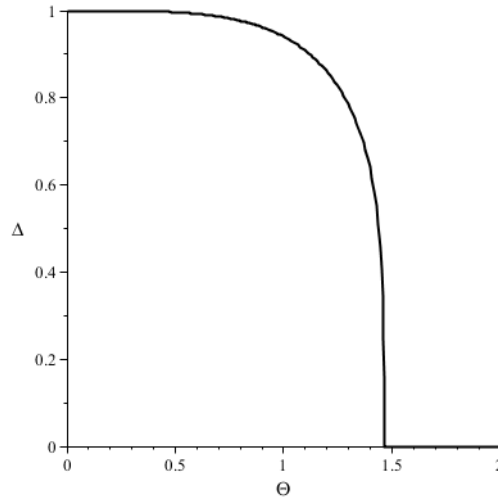


Fig. 2 The energy gap versus temperature (arbitrary units).

Typical temperature patterns of the resistance $r = R(T)$ and the thermal function $h_{TES}(T)$ in the absorber are schematically plotted in Fig. 3, in arbitrary units.

A thermal dependence describing the specific heat function may be approximately given by the formula [7]:

$$h_{JJ}(\Theta) = \begin{cases} y\gamma_{JJ}T_{c,JJ} \exp(-1,76T_{c,JJ} / \Theta), & \Theta \leq T_{c,JJ}; \\ \gamma_{JJ}\Theta, & \Theta > T_{c,JJ}, \end{cases} \quad (2.3)$$

where the value y is determined by the following condition:

$$(c_{es} - \gamma_{JJ}T_{c,JJ}) / (\gamma_{JJ}T_{c,JJ}) = 1,43. \quad (2.4)$$

Here c_{es} is the heat coefficient in the vicinity of the superconducting edge, while γ_{JJ} denotes the heat coefficient at ambient temperatures; $T_{c,JJ}$ denotes the critical temperature. The formula describing the function $h_{TES}(T)$ is completely analogous to the above expressions (though $T_{c,TES}$ is used instead the temperature $T_{c,JJ}$, and so on, all the related indexes are changed, as well).

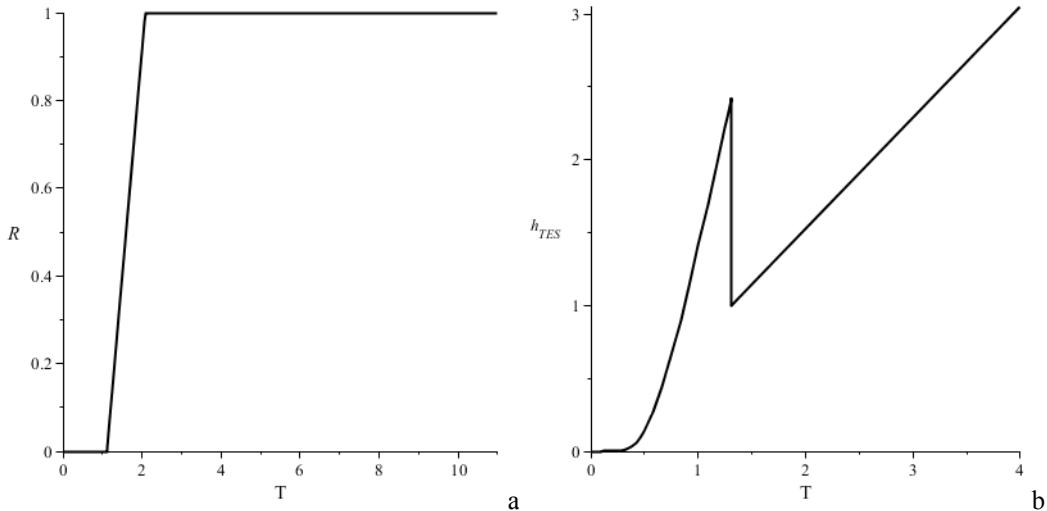


Fig. 3 Typical temperature patterns (a – resistive element; b – heat capacity).

Let us now suppose that the bolometer runs in the idle regime. Also, we neglect the temperature effects. Therefore, an approximate analytical solution to the set (2.2) may be represented by the form:

D.A. Kovriguine

$$j(t) = \Omega a_1 \cos(\Omega t + \alpha); \quad q(t) = ci\rho + a_1 \sin(\Omega t + \alpha); \quad (2.5)$$

$$v(t) = i\rho + \Omega a_2 \cos(\Omega t + \beta); \quad \varphi(t) = \Omega t + \frac{2ea_2 \sin(\Omega t + \beta)}{\hbar}.$$

where $\Omega = 2ei\rho/\hbar$ denotes the frequency generated by the Josephson junction in the absence of the resonant circuit. So that the phases and amplitudes are defined by the following equations:

$$\begin{aligned} \Omega^2 a_2 \sin(\beta) + \frac{\Omega a_1 \cos(\alpha)}{C} + \frac{\Omega a_2 \cos(\beta)}{C\rho} &= 0; \\ -\Omega^2 a_2 \cos(\beta) - \frac{\Omega a_1 \sin(\alpha)}{C} - \frac{\Omega a_2 \sin(\beta)}{C\rho} + \frac{J}{C} &= 0; \\ -\Omega^2 a_1 \cos(\alpha) - \frac{r\Omega a_1 \sin(\alpha)}{l} + \frac{a_1 \cos(\alpha)}{lc} + \frac{\Omega a_2 \sin(\beta)}{l} &= 0; \\ \frac{r\Omega a_1 \cos(\alpha)}{l} - \Omega^2 a_1 \sin(\alpha) - \frac{\Omega a_2 \cos(\beta)}{l} + \frac{a_1 \sin(\alpha)}{lc} &= 0. \end{aligned} \quad (2.6)$$

Solutions to these equations tend to be more accurate as the critical current is less than that of the bias.

Let us assume now that the generation frequency Ω is close to the natural frequency of the resonant circuit $\omega = 1/\sqrt{lc}$. Then, solutions to the set (2.6) demonstrate typical behaviors of a dynamical system near the resonance. Figure 4 displays a numerical example at the frequency $\Omega = 0,254E+11$ Hz, provided that the resistance, $r = 1,160E-03 \Omega$, is small enough. The dimensionless frequency detuning in this figure is normalized to unity with respect to the generation frequency Ω . The dimensionless amplitude a_1 is normalized by the value $ci\rho = 1,295E-15$ C, while the amplitude a_2 – by $i\rho/\Omega = 3,291E-16$ Wb.

As we can see the resonant excitation alters significantly the phase and amplitude dependences at small variations near the resonance at the point $\omega/\Omega = 1$, so that this model leads us to an idea of a sensitive sensor.

First, consider the time history of the process governed the set (2.2) at the initial conditions:

$$\varphi(0) = 0; \quad v(0) = 0; \quad j(0) = 0; \quad T(0) = T_s - \Delta T; \quad \Theta(0) = T_s - \Delta T.$$

The calculation uses the following dimensionless variables:

$$\tau = \omega t; \quad G(\tau) = j(t)/i; \quad \Phi(\tau) = \varphi(t); \quad Q(\tau) = q(t)/i\rho c; \quad G(\tau) = 2ev(t)/\hbar\omega.$$

Concrete numerical parameters are shown in the Table 1. These are taken as typically encountered ones when tracing references listed in the bibliography in an attempt to rely already achieved level in technologies. The oscillatory patterns are shown in Fig. 5.

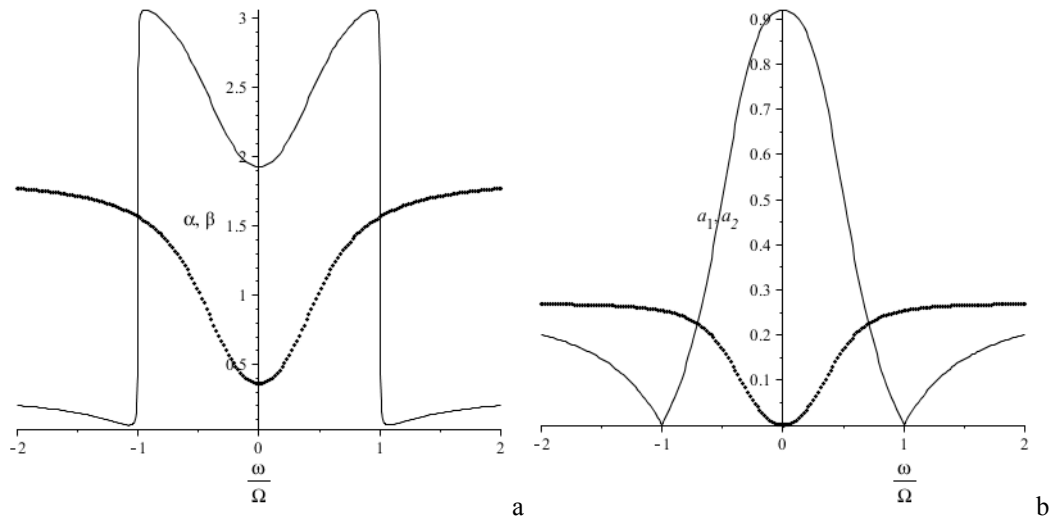


Fig. 4 Phase and amplitude response versus the frequency detuning (a –parameters α and β ; b – the parameters a_1 and a_2). Dots correspond to the parameters a_1 and α .

3. Sensor Model

As we can expect, the dynamical system representing a terahertz generator integrated with the resonant RLC–circuit, should be very sensitive to changes in the resistance r , as the circuit is tuned in the resonance with the generator. This property can be used to identify small incoming signals.

Figure 6 shows a scheme of the sensor with TES–type resistor (TES – transition edge sensors) included in the oscillatory circuit parallel to the generator, where the resistance strongly depends upon the temperature: $r = R(T)$ (Fig. 2a). In order to detect weak infrared signals, the magnetic flux near the inductive element may be measured with the help of a quantum interferometer.

Table 1

Parameters	Values	Parameters	Values
J	8,362 A	$T_s = T_{s, TES}$	0,270 K
c	1,549 F	$T_{s, JJ}$	0,030 K
i	8,362E-05 A	V_{TES}	10E-20 m ³
r	1,162E-03 Ω	Σ_{TES}	2,5E+9 W/K ⁵ m ³
l	10E-13 m	γ_{TES}	6,9E-5 Ws/K ² m ³
ρ	7,872E-10 Ω	V_{JJ}	10E-16 m ³
C	1,4E-11 F	Σ_{JJ}	2,5E+9 W/K ⁵ m ³
		γ_{JJ}	6,9E-5 Ws/K ² m ³

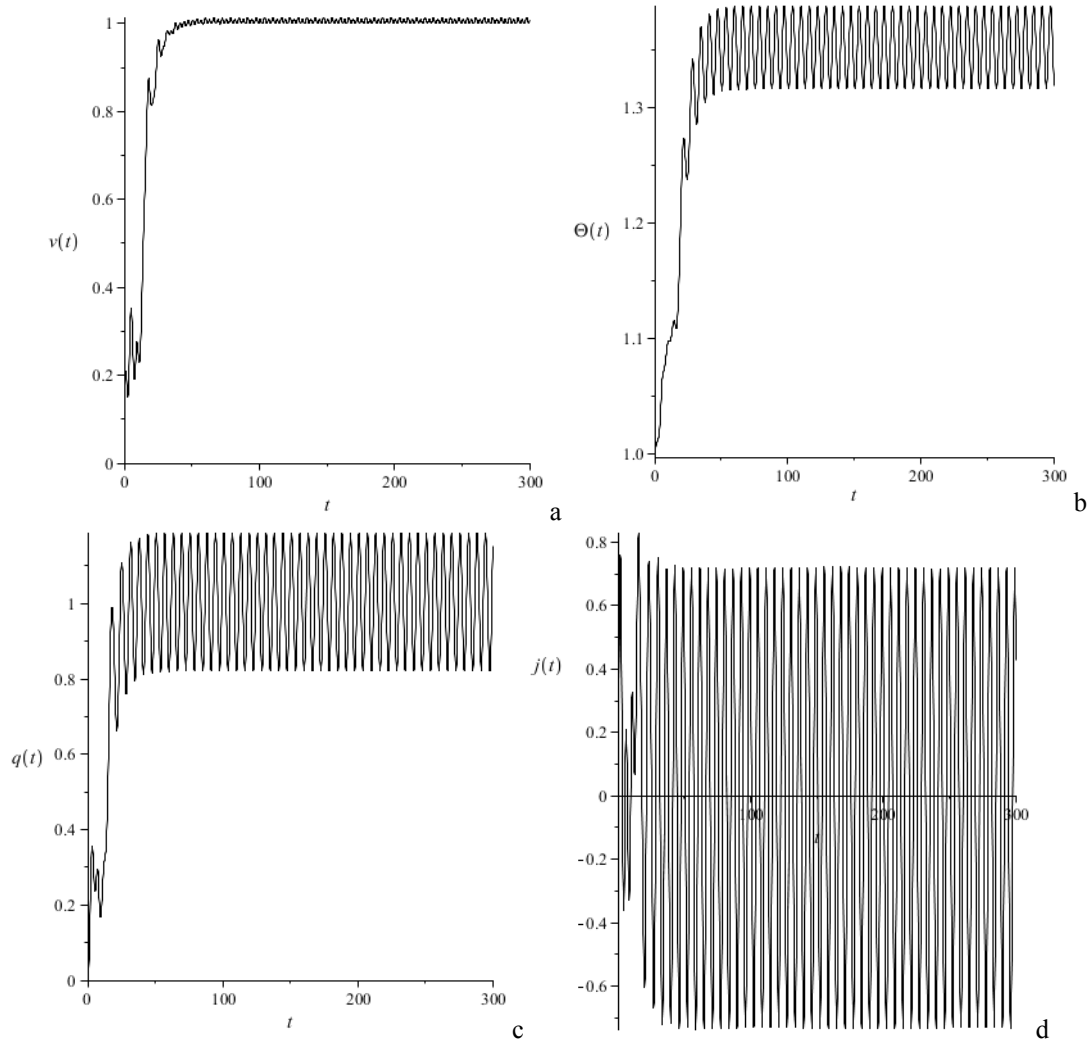


Fig. 5 Dynamical response in the idle regime (a – voltage in the junction; b – temperature of the Josephson junction; c – charge in the RLC-circuit; d – current in the RLC-circuit).

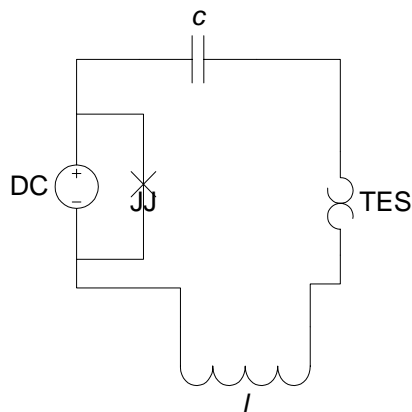


Fig. 6 Self-excited resonant bolometer.

Accordingly to the scheme shown in Fig. 6, the following equations are derived by modifying the set (2.2), when taking into account the resistance of TES-type:

D.A. Kovriguine

$$C\dot{\nu} + \nu / \rho + J \sin \varphi = i - j; \quad \dot{\varphi} = 2e\nu / \hbar;$$

$$V_{TES} h_{TES} \dot{T} = R(T) j^2(t) - V_{TES} \Sigma_{TES} \left[T^n - (T_s - \Delta T)^n \right] + P(t); \tag{3.1}$$

$$V_{JJ} h_{JJ} \dot{\Theta} = (i - j) \nu - V_{JJ} \Sigma_{JJ} \left[\Theta^n - (T_s - \Delta T)^n \right]$$

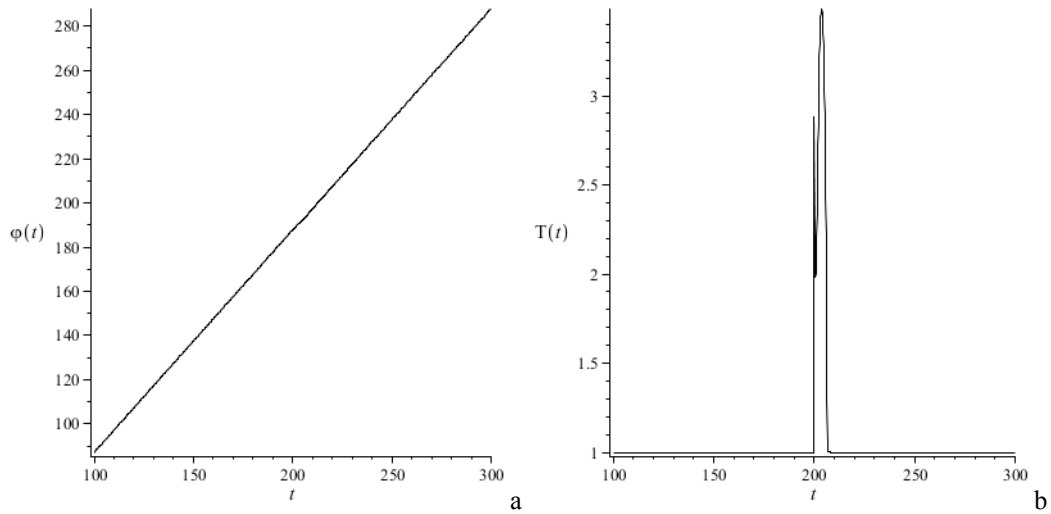
$$\dot{j} + q / c + R(T) j = \nu; \quad \dot{q} = j.$$

in which $P(t)$ is the external power. The remaining notations are the same. In contrast to the model (2.2), the set (3.1) cannot be subject to effective analytical study. In this case one may rely to numerical calculation only. In order to test the dynamics governed by the model (3.1), we use the parameters in Table 1. The external pulse is supposed to have a rectilinear profile, and let Δt be characteristic pulse duration over the time. The additional parameters are shown in Table 2:

Table 2

Parameters	Values	Parameters	Values
R	11,600 Ω	$R_r T / R$	50
P	10E-13 W	Δt	10E-13 s

The results are presented in Fig 7. The same dimensionless variables are utilized. It is obvious that the absorption of the external pulse can be clearly observed due to dynamical changes in the amplitude and phase. In particular, one can see that the time point corresponding to the pulse absorption is characterized by almost zeros of the current and voltage. This means that the model of the self-excited resonant bolometer possesses an effective feedback which creates most optimal conditions for a quickest sensor cooling. This would lead to a technical result which should improve the sensitivity, accuracy and stability of the sensor by reducing the measurement errors up to the level restricted by thermal fluctuations. This lends us more efficient identifying of unknown parameters of incoming electromagnetic signals.



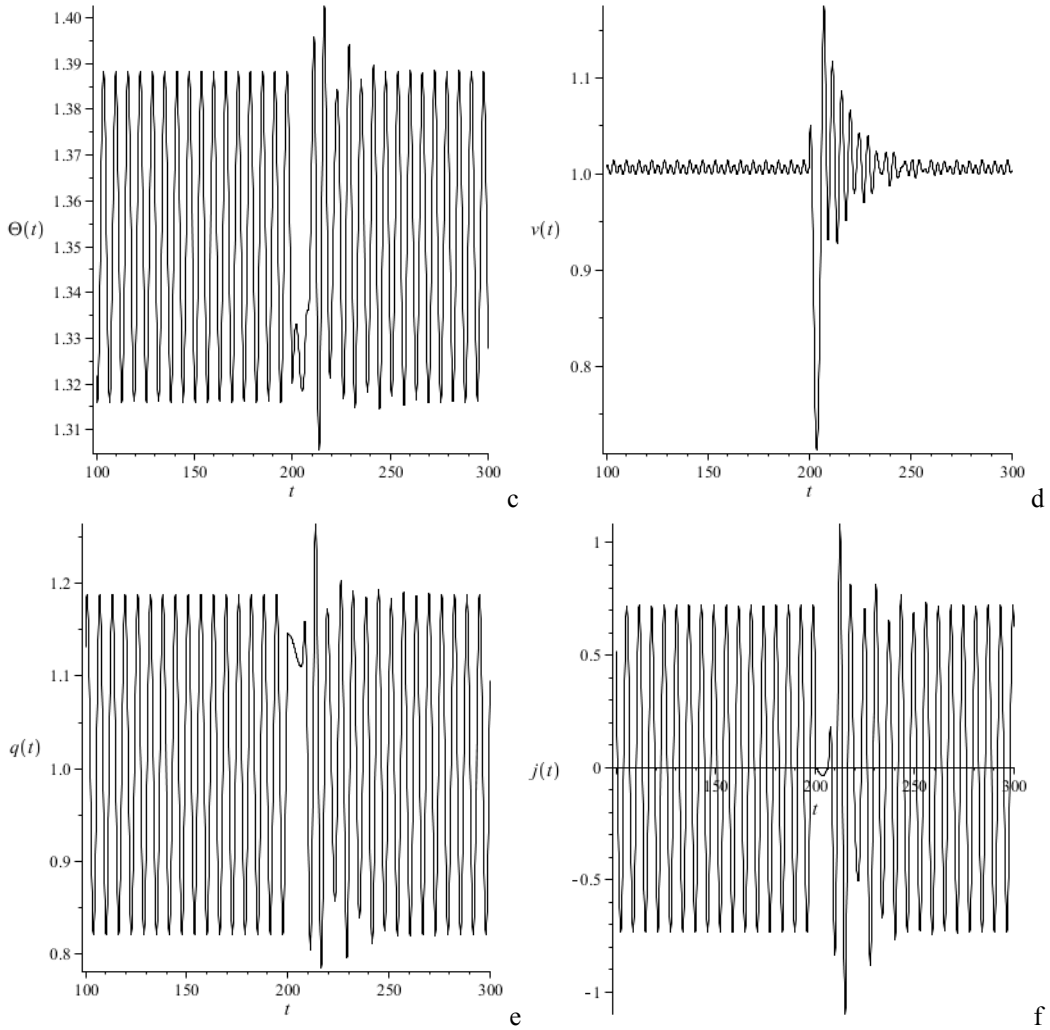


Fig. 7 Bolometer dynamics (a – Josephson phase; b – temperature of the resistive element over the time; c – temperature of the junction; d – voltage; e – charge; f – current). The pulse comes at the time of 200 dimensionless units.

Finally, the physical processes in the self-excited resonant bolometer may be consumed by the following elementary acts. The low-noise high-frequency generator of oscillations is represented by a terahertz Josephson junction, which is loaded by the resonant RLC-circuit in parallel. The inductive element of the circuit allows for an accurate readout from the sensor with the help of a quantum interferometer. The frequency of electric oscillations is generated in the circuit at the same frequency as that of emitted electromagnetic waves in the case of the critical biasing. Let the resonant circuit be tuned into the resonance with the Josephson generator, and then the maximal loading is provided. This resonance is accompanied by decreasing in the amplitude of oscillations in the generator, while the amplitude increases in the circuit at the same time. The resonance creates stationary self-excited oscillatory regimes, which exhibit stable patterns at terahertz frequencies. If the sensor is out of balance, because of the absorption of the external pulse, then the negative feedback reacts extremely quickly to return the sensor to its original unperturbed state.

4. Noise-equivalent power

If the temperature of the physical body is above the absolute zero, then there are always present thermal fluctuations [13, 14]. The main objective is that these fluctuations have to be small compared to the useful signal. The noise-equivalent power due to the electron scattering on phonons is estimated by the following standard formulae:

$$NEP_{TES} = 20k_B V_{TES} \Sigma_{TES} T^6(t); NEP_{JJ} = 20k_B V_{JJ} \Sigma_{JJ} \Theta^6(t) \quad (4.1)$$

D.A. Kovriguine

The estimations of noise generated at the electron scattering caused by the resistance reads:

$$NEV_r = 4rk_b T(t); \quad NEV_\rho = 4\rho k_b \Theta(t) \quad (4.2)$$

While the evaluation of noise due to the dynamical recharge of capacitors holds true:

$$NV_c = k_b T(t)/c; \quad NV_C = k_b \Theta(t)/C \quad (4.3)$$

Therefore, the noise evaluation, for the example present in the above section, would be roughly: $NEP_{TES} = 2,425E-32 \text{ W}^2/\text{Hz}$; $NEP_{JJ} = 9,933E-31 \text{ W}^2/\text{Hz}$; $NEV_r = 5,381E-22 \text{ V}^2/\text{Hz}$; $NEV_\rho = 1,855E-23 \text{ V}^2/\text{Hz}$; $NV_c = 7,486E-13 \text{ V}^2$; $NV_C = 3,313E-13 \text{ V}^2$.

Let us consider the dimensionless transient process in the bolometer, accordingly to the time history shown in the previous section. We can observe typical time duration, about 100 dimensionless units, i.e. the physical time interval is $2,473E-9 \text{ s}$ (Fig 7c). This means that the frequency band width can be estimated as about $4,044E+8 \text{ Hz}$. Therefore, the noise, accordingly to the above formulae, should be of the order $10E-13 \text{ W}$ by the power, and $10E-8 \text{ V}$ – by the voltage. Since the noise has the same order as the power of the external pulse P , related to the numerical example, we have evaluated a sensitivity threshold of the bolometer to infrared signals. Finally, the interested reader can trace in detail all the numerical examples used in this study [15].

5. Conclusions

The reliability of the mathematical model describing dynamical operating regimes in the self-excited resonant bolometer may be confirmed by many recent successes in nanotechnologies, referred in the references. In addition, the patent US8063369 uses several interconnected in a cascade TES-type sensors providing a very sharp response of the bolometer. The main difference of this prototype from the self-excited resonant bolometer is that a constant bias voltage is used to power the cell of detectors. Note that the constant bias, either the current or voltage, would naturally limit the effectiveness of the feedback which should promote a rapid cooling of the detector up to the operating point. Unlike this, the self-excited resonant bolometer has a variable biasing, both in the current and voltage. This supports some fruitful conditions for the feedback properties to reduce the time constant of the bolometer.

Let us consider the effectiveness of resonant circuits in the exciting design of bolometers. A sensitive element in the resonant circuit may play the role as a capacitor or inductor. An example can be found in the patent US6534767. It is well known that the capacitance or inductance both depend on the ambient temperature, which affects changes in the impedance. This causes variations in the resonant frequency which may be registered through the phase-locked loops. The main deficiency of such a prototype is that it uses ferroelastic materials, which are able to exhibit the desirable qualities at relatively high temperatures only, and therefore, this cannot provide accurate measurements because of thermal noises.

A low-noise high-frequency generator of oscillations in the resonant bolometer can be represented by a terahertz Josephson junction, as the best candidate. In particular, the patent US8026487 describes a superconducting tunable coherent terahertz generator based on the resonant coupling between the Josephson oscillations and the fundamental mode of the cavity resonator, which leads to a powerful terahertz radiation. Let this generator be loaded by the resonant RLC-circuit in parallel [16]. The junction, at the critical biasing, generates a localized electromagnetic radiation. The frequency of electric oscillations in the circuit is the same as that of emitted electromagnetic waves. Then, the resonant circuit may be tuned into the resonance with the Josephson generator to provide the maximal loading. The resonance creates stationary self-excited oscillatory regimes, which are stable at terahertz frequencies.

Note that the self-excited resonant bolometer represents a mesoscopic device. Then the efficiency is restricted by geometrical dimensions of the system. The mathematical description represented in this paper is based on the semi-classical physical methods. Let the dimensions decrease with the increasing the purity of a sensor material, then the bolometer turns into a typical quantum system. It is possible that perspective sensor elements can be composed of monatomic metallic layers covered by graphene sheets. This would ensure a minimization of the heat capacity. Graphene, accordingly to the state-of-the-art, exhibits extremely high thermal properties which should maximize the thermal conductivity. To implement such elements in the bolometer one may

pay attention on new intercalation technologies [17], NEMS terahertz resonators are also of higher interest [18]. The permanent evolution in nanotechnologies would provide the appearance of very rapid and efficient devices such as quanta counters. Such devices would be manifested as intently quantum objects. However, their manufacturing, but not only the mathematical description, seems to be not so easy tasks [19].

References

1. Mazin B.A., Bumble B., et al., 'Position sensitive x-ray spectrophotometer using microwave kinetic inductance detectors', *Appl.Phys.Lett.*, **89** (2006), 222507–222510.
2. Day P., LeDuc H., et al., 'A broadband superconducting detector suitable for use in large arrays', *Nature*, **425** (2003), 817–820.
3. Shitov S.V., 'Bolometer with high-frequency readout for array applications', *Tech.Phys.Lett.*, **37(10)** (2011), 932–934.
4. Segev E., Suchoi O., et al., 'Self-oscillations in a superconducting strip-line resonator integrated with a DC superconducting quantum interference device', *Appl. Phys. Lett.*, **95** (2009), 152509–152511.
5. Vijay R., Devoret M.H., Siddiqi I., 'The Josephson bifurcation amplifier', *Rev. Sci. Instrum.*, **80** (2009), 111101–111118.
6. Josephson B.D., 'Possible new effects in superconductive tunneling', *Phys. Lett.*, **1** (1962), 251–253.
7. Feynman R.P., Leighton R.B., Sands M., 'The Feynman Lectures on Physics, Volume 3: Quantum Mechanics', Massachusetts: Addison-Wesley, Reading, 1965.
8. Ginzburg V.L., 'On superconductivity and superfluidity (what I have and have not managed to do), as well as on the 'physical minimum' at the beginning of the XXI century (December 8, 2003)', *Physics-Uspeski*, **47(11)** (2004), 1155–1170.
9. Cooper L.N., 'Bound electron pairs in a degenerate Fermi gas', *Phys. Rev.*, **104** (1956), 1189–1190.
10. Bardeen J., Cooper L.N., Schrieffer J.R., 'Microscopic theory of superconductivity', *Phys. Rev.*, **106**(1957), 162–164.
11. Bardeen J., Cooper L.N., Schrieffer J.R., 'Theory of superconductivity', *Phys. Rev.*, **108(5)** (1957), 1175–1204.
12. Buckingham M.J., 'Schematic diagram of the apparatus for infrared measurements', *Phys. Rev.*, **101** (1956), 1431–1432.
13. Johnson J.B., 'Thermal Agitation of Electricity in Conductors', *Phys. Rev.*, **32** (1928), 97–109.
14. Mather J.C., 'Bolometer noise: nonequilibrium theory', *Appl. Opt.*, **21(6)** (1982), 1125–1134.
15. <http://kovriguineda.ucoz.ru/index/bolometer/0-31>
16. Tachiki M., Ivanovic K., Kadowaki K., 'Emission of terahertz electromagnetic waves from intrinsic Josephson junction arrays embedded resonance in LCR circuits', *Phys. Rev. B* **83** (2011), 014508–014515.
17. Riedl C., Coletti C., et al., 'Quasi-free-standing epitaxial graphene on SiC obtained by hydrogen intercalation', *Phys. Rev. Lett.*, **103** (2009), 246804–246807.
18. Yuehang Xu, Changyao Chen, et al., 'Radio frequency electrical mechanical transduction of graphene resonators', *Appl. Phys. Lett.*, **97** (2010), 243111–243113.
19. Nakamura Y., et al., 'Control of coherent macroscopic quantum states in a single-Cooper-pair box', *Nature*, **398** (1999), 786–788.